


Study on temperature response of the HERD calorimeter cell

Yingying Dai^{1,2} · Xingzhu Cui²  · Xin Liu² · Yongwei Dong² · Hongwei Liang³ · Zhenzhong Zhang³ · Xiaochuan Xia³ · Zhipeng Wei¹

Received: 23 September 2022 / Revised: 13 December 2022 / Accepted: 20 December 2022 / Published online: 6 January 2023
© The Author(s), under exclusive licence to Institute of High Energy Physics, Chinese Academy of Sciences 2023

Abstract

Purpose To derive the temperature response of the basic unit of the electromagnetic calorimeter of the high energy cosmic-radiation detection (HERD) facility.

Method Tested a method to measure HERD calorimeter cell (HCC) light yield using an ultraviolet Light-Emitting Diode with a wavelength of 300 nm, and established an experimental setup and tested the light yield of the HCC at different temperatures in a thermal chamber.

Results and conclusions The result showed that the signal amplitudes variation of the HCC reached up to 10.2% with temperature ranging from 0 to 60 °C, if we narrow the temperature range to 0–35 °C, the variation was about 3.7% and it showed much better linearity. This result provides a good instruction on the thermal control of the HERD calorimeter (CALO) to improve its performance.

Keywords HERD · LYSO · WLSF · Optical output · Temperature response

Introduction

HERD is a planning flag-ship mission in high energy astrophysics built by an international collaboration with contributions from China, Italy, Switzerland, and Spain. The key science objectives of HERD can be summarized as: probing the evidence of dark matter, precisely measuring cosmic rays spectrum and composition up to the knee region, and surveying gamma-ray sources [1].

As the primary instrument of HERD, the CALO is designed to be an imaging, wide field-of-view (FOV), high-energy range lutetium–yttrium oxyorthosilicate (LYSO) array, covering the energy range from 30 GeV to more than 1

PeV [2]. The CALO will be composed of about 7500 HCCs. Each HCC consists of a LYSO crystal cube and a readout pad with a pair of rolled wavelength shifting fibers (WLSF), the size of the crystal is $3 \times 3 \times 3 \text{ cm}^3$, which is shown in Fig. 1. The CALO measures the tracks of the energetic particles induced by an incident high energy particle undergoes electromagnetic showers or hadron showers in the LYSO crystal array. The energies of the subsequent electromagnetic showers are also recorded [3, 4].

As both the performances of the LYSO crystals, such as luminescence efficiency, luminescence decay time, optical attenuation length, and the optical transmission efficiency of the WLSF, are related to the temperature [5–7], and all of them are negatively correlated with temperature [7, 8], so the signal amplitude of HCC will be different as the ambient temperature changes. While the stability of the HCC signal is of much importance to precisely reconstruct the incident particles, it is important to derive the relationship between signal amplitude and ambient temperature, so that we can constrain the signal amplitude in a limited range by controlling the temperature of the CALO array.

An experimental setup was established with a temperature chamber, a cube cell composed of a LYSO crystal, a WLSF pad, a 300 nm LED and a photomultiplier tube (PMT). Both the PMT and the LED were placed outside

✉ Xingzhu Cui
cuixingzhu@ihep.ac.cn

✉ Zhipeng Wei
zpweicust@126.com

¹ State Key Laboratory of High Power Semiconductor Lasers, Changchun University of Science and Technology, Changchun 130022, China

² Institute of High Energy Physics, Chinese Academy of Sciences (CAS), Beijing 100049, China

³ School of Microelectronics, Dalian University of Technology, Dalian 116024, China

Fig. 1 The scheme of a HERD Calorimeter Cell. The crystal was wrapped with Enhanced Specular Reflector (ESR), and the above is WLSF pad, which is tightly attached to the crystal



the chamber to exclude the temperature effect on them, See detail in Sect. "Optical output temperature response of the calorimeter unit". The relationship between HCC signal and ambient temperature was obtained with a temperature range from 0 to 60 °C. The result showed that the variation was about 10.2% with temperature ranging from 0 to 60 °C, if we narrow the temperature range to 0–35 °C, the variation was about 3.7% and it showed much better linearity. It is valuable data for the thermal control design of CALO.

Determination of exciting source of LYSO Scintillator

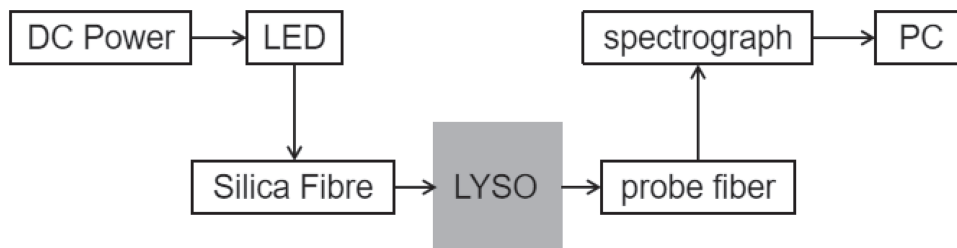
As a traditional method to induce the fluorescence of scintillation crystals [9], the X-rays source has the disadvantage of imposing radiation hazards to the testing crew, and it is much difficult to guide X-ray beam outside the chamber to crystal inside the chamber, if put X-ray source inside the chamber, the intensity of X-ray would vary with the temperature, but it is easy to feed the UV light outside the temperature chamber and into the chamber with guiding silica fiber. So, to find a safe and simple experiment system, in this research, we tried

to replace the X-ray source with an ultraviolet LED as an incident source for the LYSO crystal [10].

To verify the feasibility and rationality of the exciting source, we investigated the fluorescence spectrum of the crystal induced by the 300 nm LED and compared it with the spectrum induced by an X-ray source. The scheme of spectrum measuring is shown in Fig. 2. The LED was driven by a DC power source, and the ultraviolet lights generated by LED were transmitted to the crystal surface through a guiding silica fiber. The fluorescence spectrum of LYSO crystal excited by the incident ultraviolet lights was collected by the Thorlabs CCS200 spectrometer.

LYSO crystal has two crystallographically independent lutetium sites. When it is doped with Ce, the dopant Ce occupies two different sites and thus the existence of two activation centers (called "Ce1" and "Ce2"). As shown in Fig. 3, it can be seen that the main luminescence peak of the crystals are all around 425 nm in this two excitation modes. But the X-ray fluorescence spectrum is softer than the LED one, which may be caused by the difference of excitation mechanism of the two excitation source, the excitation

Fig. 2 Experimental block diagram of the measurement of fluorescence spectra of LYSO crystals



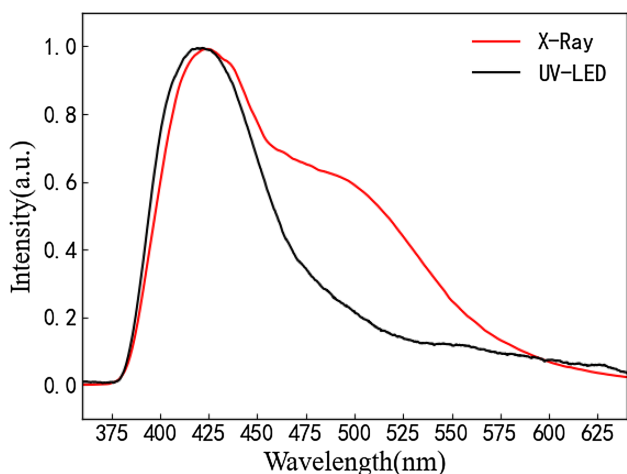


Fig. 3 Fluorescent spectra of LYSO crystals excited by LED and X-ray, respectively. Red is the fluorescence spectrum of LYSO excited by X-ray, and black is the fluorescence spectrum of LYSO excited by 300 nm LED

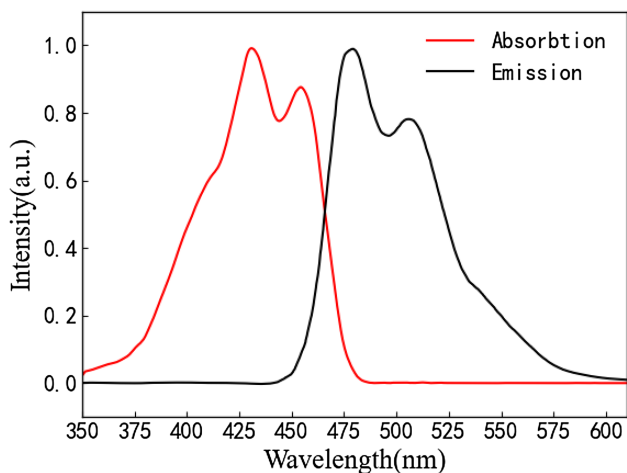
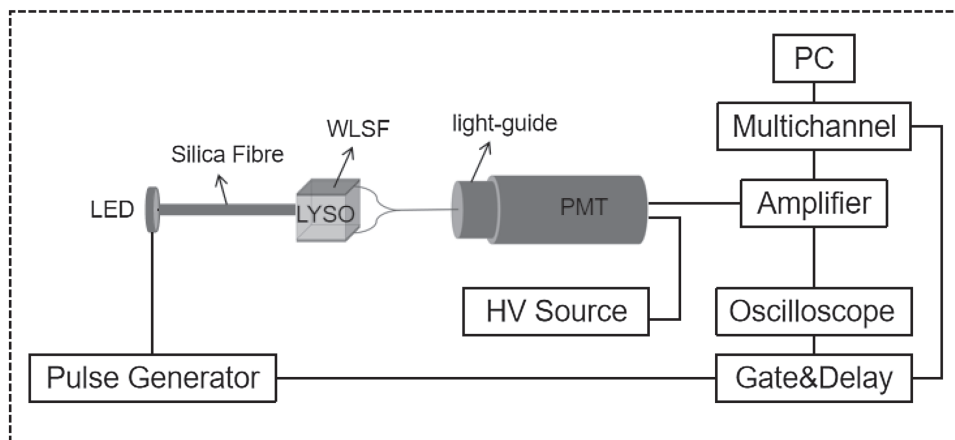


Fig. 4 The absorption and emission spectra of the WLSF

Fig. 5 Schematic diagram of the experimental principle of the optical output temperature response of the HCC



wavelength of 300 nm LED, corresponding to the strongest Ce1 excitation band with emission peak appear at 425 nm, and the excitation of X-ray corresponds to another excitation modes: Ce1 and Ce2 excited together [11–13].

The UV light was used as an incident source to derive the temperature dependence of Ce-doped rare-earth Crystal in former work [14]. And combined with the absorption and emission spectra of the WLSF, as shown in Fig. 4, that the main absorption peak of WLSF is at 425 nm, it can coincide with the crystal main luminescence peak, but it is not capable to absorb light around 500 nm produced by X-ray excitation. So, although it does not have a luminescence peak of 500 nm produced when using the LED excitation, this should have little effect on the temperature response of the HCC. Given the above-mentioned information, it is reasonable and convenient to adapt 300 nm LED as an excitation source.

Optical output temperature response of the calorimeter unit

Experimental setup

As shown in Fig. 5, a 300 nm LED was driven by a pulse generator (BNC Model PB-5), then the emission light of the LED was guided onto the LYSO crystal by a ~1.0 m silica optical fiber. The photograph of the guiding silica fiber is shown in Fig. 6. The signal from the scintillating crystal is read out with a WLSF pad adhered to the HCC. The diameter of WLSF is 0.3 mm and the pad was equipped with two ~3.6 m long WLSFs coiled into different turns which carried the light from the crystal to an acrylic light guide. In the light guide, the light from four ends of the WLSFs are merged onto a single photomultiplier tube (PMT XP-2020). The PMT was biased by a high-voltage supply (CAEN. N470). The negative signals from PMT were amplified by a shaping amplifier (ORTEC 572A). The outputs from

Fig. 6 The photograph of the guiding silica fiber



the amplifier were digitized by the multichannel analyzer (Amptek MCA8000D) to obtain the pulse height spectrum.

The active scintillating crystal is produced by Beijing Hamamatsu Photon Techniques Inc, while the Y-11 type WLSF was manufactured by Kuraray (Japan). To increase the light collecting efficiency, the HCC was wrapped with ESR [15]. To achieve much better noise suppression, the signal of the pulse generator was also input to a gate and delay generator (ORTEC 416A) to generate a gate signal, with a delayed and broadened gate signal, the amplified signal in coinciding with the pulse signal driving the LED were picked out.

Experimental process

To derive reliable data, the experimental setup is tested in the laboratory with normal temperature and pressure. After multiple debugging, the final experimental parameters are set as follows: The pulse generator output voltage is 7.5 V, pulse rising time is 50 ns, falling time is 500 ns, flat top is 150 ns, the pulse frequency is 201 Hz; the bias for PMT is 1900 V; the gain for shaping amplifier is 100, and the shaping time is 2 microsecond; the integration time of multichannel analyzer is 600 s. It can be obtained a stable fluorescence signal and the signal will be easily collected by system in these experimental parameters.

Multiple tests were conducted at room temperature with room temperature of 25 °C. The derived pulse height spectra were fitted with Gaussian distribution, the peaks position of Gauss model were extracted as the corresponding energy amplitude. Figure 7 shows the energy channel value of four hours consecutive tests at room temperature. As shown in the figure, because the PMT has a certain work stability

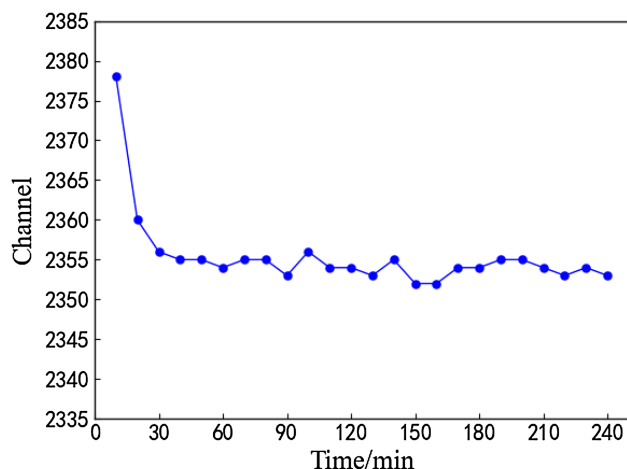


Fig. 7 The energy channel value of four hours consecutive tests at room temperature

time when starting the work, during the first 30 min of the experiment, the measured energy amplitude varies greatly. After 30 min, the variation in the spectrum is not obvious, which ensures that the data are reliable. By fitting the data with a linear equation, the derived error in peak centers of the tests is only about 0.83%.

The temperatures range from 0 to 60 °C were chosen as the setting ambient temperatures. The HCC was placed in a temperature chamber (CTE-SE7512-05F) to obtain the temperature response of the cube. The LED, the pulse generator, the PMT and all the other electronic instruments were all placed outside of the chamber to exclude the temperature effect on them. As mentioned above, the emitted light of LED was guided onto the LYSO crystal surface by a silica

optical fiber. The ambient temperatures were read from the screen of the chamber, while the temperatures of the cube were derived from the temperature probes pasted on the surface of the cube. To ensure that the crystal can reach thermal equilibrium at a setting temperature, the data acquisition of the pulse height spectrum started when the temperature on the crystal surface remained unchanged for 30 min. The whole experimental setup is shown in Fig. 8.

To reduce the experimental error from all possible sources, five sets of data were tested for each temperature point, and the measured data of each set were fitted in Gaussian to obtain the coordinates of the peak position, and took the average of the five sets of peak positions as the corresponding energy channel value of each temperature point.

In addition, in order to avoid the influence of PMT instability on the experiment, no data was collected 30 min before the experiment, and the voltage of PMT is not closed during the experiment to make it always in the working state.

Data analysis

Thirteen temperatures range from 0 to 60 °C were chosen as the setting ambient temperatures, as listed in Table 1. During the experiment, the preset temperature and ambient temperature of the chamber remained stable, while the temperature variety of the cell did not exceed 0.1 °C within the data acquiring duration. At each temperature



Fig. 8 Photograph of the experimental setup of temperature response of the HCC

Table 1 The pulse heights measured at the setting temperatures

Text-box temperature (°C)	Crystal surface temperature (°C)	Pulse height					Average	Absolute error (±)
		1	2	3	4	5		
0.0	0.1	2408	2404	2404	2405	2405	2405.2	2.8/1.2
5.0	5.0	2385	2387	2383	2384	2383	2384.4	2.6/1.4
10.0	10.1	2379	2378	2377	2378	2378	2378.0	1.0/1.0
15.0	14.9	2377	2376	2375	2377	2376	2376.2	0.8/1.2
20.0	20.0	2357	2358	2358	2357	2357	2357.4	0.6/0.4
25.0	25.0	2353	2354	2355	2355	2356	2354.6	1.4/1.6
30.0	29.9	2330	2331	2329	2330	2330	2330.0	1.0/1.0
35.0	35.0	2315	2313	2311	2312	2312	2312.6	2.4/1.6
40.0	39.9	2278	2278	2279	2279	2278	2278.4	0.6/0.4
45.0	44.9	2266	2266	2267	2267	2267	2266.6	0.6/0.4
50.0	50.0	2232	2232	2231	2232	2232	2231.8	0.2/0.8
55.0	55.0	2208	2209	2210	2209	2209	2209.0	1.0/1.0
60.0	59.9	2155	2155	2156	2156	2155	2155.4	0.6/0.4

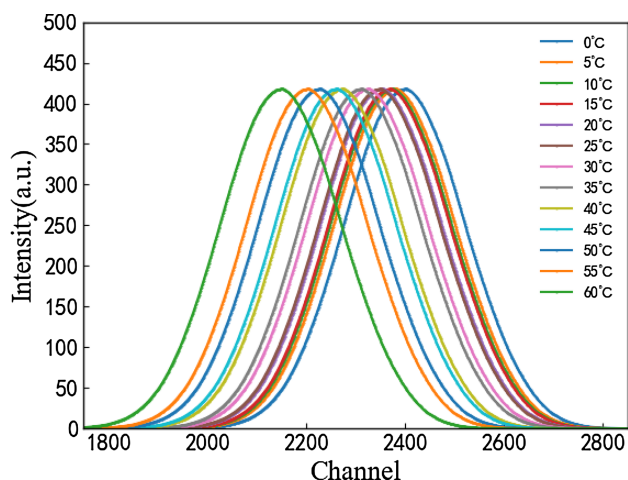


Fig. 9 Pulse height spectrum of different ambient temperature

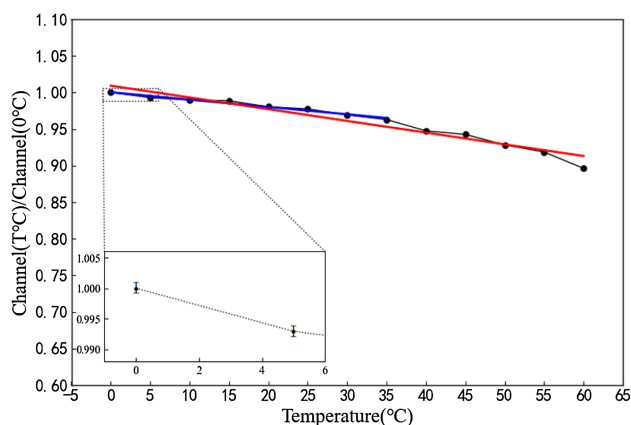


Fig. 10 Energy channel value at each temperature and linear fitting. The red line is the normalized energy channel value and linear fitting in the range of 0 °C to 60 °C; the blue line is the normalized energy channel value and linear fitting in the range of 0 °C to 35 °C

point, five pulse height spectra were derived, so that both the average of the pulse height and the absolute error of the pulse height could be obtained.

The pulse height spectra of different temperature were compared as shown in Fig. 9. As the temperature increases, the measured pulse height decreases, which indicates that the light yield of HCC is negatively correlated with temperature.

To quantitatively analyze the difference in light yield of HCC in different ambient temperature, the pulse height values were normalized to the one measured at 0 °C. As it can be seen in Fig. 10, the reduction of light yield is about 10.2% when the temperature increases from 0 °C to 60 °C. The temperature dependence of the HCC can be fitted with a linear function:

$$P_{\text{HCC}} = -0.00170 T + 1.0092$$

where P_{HCC} is the pulse height values were normalized to the one measured at 0 °C, and T is the temperature of the HCC in °C.

However, the fitted linear correlation coefficient R^2 is only 0.98341, and the fitting effect was not very good. When the temperature is greater than 35 °C, we can see that the curve has a significant downward trend, if the temperature range is confined to 0 °C ~ 35 °C, the reduction in light yield is about 3.7%. The temperature dependence of the HCC shown in Fig. 10 can be fitted with a linear function:

$$P_{\text{HCC}} = -0.00106 T + 1.0003$$

The fitted linear correlation coefficient, R^2 , was improved to 0.99857. It is observed that in the temperature range of 0 °C to 35 °C, the light output intensity basically changes linearly, and we can estimate a light yield decreasing rate of ~1% for 10 °C temperature variation for HCC.

This result is different from previous temperature response results of luminescence efficiency of LYSO crystal or the optical transmission efficiency of the WLSF alone, as the WLSF was designed specified for the HERD, there is no similar design to be compared with. And the preliminary test on LYSO Crystal test, it is not consistent with the reference, which can be caused by the manufacturing technologies. Meanwhile, the different temperatures may also affect the coupling states of LYSO and WLSF pad. So, the specific reasons remain to be studied and here we only study the temperature response of the couple bodies of LYSO and WLSF pad.

Conclusion

A method to measure HERD HCC light yield using an ultra-violet LED with a wavelength of 300 nm was tested in this work. The reliability of this method was proved by comparing the fluorescence spectrum excited by X-ray and the 300 nm LED.

Based on this, we established an experimental setup to derive the pulse height variation of HERD HCC with ambient temperature. With the thirteen measurements of temperature ranging from 0 to 60 °C, the relationship between the light yield and the ambient temperature was obtained. With the derived data, we can draw the following conclusion: (1) the light yield of HCC decreases with increasing temperature. (2) The reduction in light yield is up to 10.2% when the temperature ranged from 0 to 60 °C. (3) If the temperature range is narrowed from 0 to 35 °C, the variation in light yield is as low as 3.7%, and the light yield and the temperature are in a good linear relationship.

The data in this work are valuable to determine the operating temperature of the HERD CALO array. If we limited the ambient temperature of CALO in range from 0 to 35 °C, we can constrain the signal amplitude in a limited range, and if we narrow down the temperature range, the variation will be lower. That is, we can limit the operating temperature in a narrow range to deduce the variation, it can reconstruct the incident particles more precisely. At the same time, it is valuable data for the thermal control design of CALO.

Acknowledgements Thank the support from the National Natural Science Foundation of China (Grant Nos. 12027803, 11875097, 11975257) and the support from the International Partnership Program of Chinese Academy of Sciences (Grant No. 113111KYSB20190020).

Declarations

Conflict of interest The authors declare that they have no conflict of interest.

References

1. C. Altomare et al., Particle identification capability of Plastic scintillator tiles equipped with SiPMs for the High Energy cosmic-Radiation Detection (HERD) facility. *Nucl Instrum Methods Phys Res Sect A: Accel Spectrom Detect Assoc Equip* **983**, 164476 (2020). <https://doi.org/10.1016/j.nima.2020.164476>
2. P.W. Cattaneo, The space station based detector HERD: precise high energy cosmic rays physics and multimessenger astronomy. *Nucl Particle Phys Proc* **306–308**, 85–91 (2019). <https://doi.org/10.1016/j.nuclphysbps.2019.07.013>
3. C. Wanarak et al., Luminescence and scintillation properties of Ce-doped LYSO and YSO crystals. *Adv Mater Res* **199–200**, 1796–1803 (2011). <https://doi.org/10.4028/www.scientific.net/AMR.199-200.1796>
4. T. Yagi et al., A small high sensitivity neutron detector using a wavelength shifting fiber. *Appl Radiat Isot* **69**(1), 176–179 (2011). <https://doi.org/10.1016/j.apradiso.2010.07.016>
5. L. Cheng et al., Temperature induced spectral lines broadening and fluorescence quenching in Tm:YAG crystals. *Acta Opt Sinica* (1999). <https://doi.org/10.3321/j.issn:0253-2239.1999.02.019>
6. Zhang T et al. (2016) Several main influencing factors of the LYSO:Ce Afterglow. *J Synth Cryst* <https://doi.org/10.16553/j.cnki.issn1000-985x.2016.07.013>.
7. Z. Zong et al., Study of light yield for different configurations of plastic scintillators and wavelength shifting fibers. *Nucl Instrum Methods Phys Res* **908**, 82–90 (2018). <https://doi.org/10.1016/j.nima.2018.08.029>
8. Kim CL (2005) A study on the temperature characteristics of LYSO PET detector. In: Nuclear science symposium conference record, IEEE vol.4. 2005, 4-. <https://ieeexplore.ieee.org/stamp/stamp.jsp?tp=&arnumber=1596728&tag=1>
9. G.V. Ioannis et al., Evaluation of the light emission efficiency of LYSO: Ce scintillator under X-ray excitation for possible applications in medical imaging. *Nucl Instrum Methods Phys Res* (2006). <https://doi.org/10.1016/j.nima.2006.08.018>
10. K. Wei et al., Photoluminescence nonlinearity and picosecond transient absorption in an LYSO: Ce scintillator excited by a 266 nm ultraviolet laser. *RSC Adv* **11**(28), 17020–17024 (2021). <https://doi.org/10.1039/D1RA00347J>
11. J.D. Naud, T.A. Tombrello, The role of cerium sites in the scintillation mechanism of LSO. *IEEE Trans Nucl Sci* **43**(3), 1324–1328 (1996)
12. C.M. Pepin et al., Properties of LYSO and recent LSO scintillators for phoswich PET detectors. *IEEE Trans Nucl Sci* **51**(3), 789–795 (2004). <https://doi.org/10.1109/TNS.2004.829781>
13. Suzuki H, Tombrello TA, Melcher CL et al (1992) Light emission mechanism of Lu₂(SiO₄)O:Ce. Nuclear science symposium and medical imaging conference, 1992. Conference Record of the 1992 IEEE. IEEE. <http://authors.library.caltech.edu/50503/1/00256584.pdf>
14. H. Suzuki, T.A. Tombrello, C.L. Melcher et al., UV and gamma-ray excited luminescence of cerium-doped rare-earth oxyorthosilicates. *Nucl Instrum Methods Phys Res Sect A: Accel Spectrom Detect Assoc Equip* **320**(1–2), 263–272 (1992). [https://doi.org/10.1016/0168-9002\(92\)90784-2](https://doi.org/10.1016/0168-9002(92)90784-2)
15. Z. Ji et al., Investigation of optical transmittance and light response uniformity of 600-mm-long BGO crystals. *Nucl Instrum Methods Phys Res A* **753**, 143–148 (2014). <https://doi.org/10.1016/j.nima.2014.03.056>

Springer Nature or its licensor (e.g. a society or other partner) holds exclusive rights to this article under a publishing agreement with the author(s) or other rightsholder(s); author self-archiving of the accepted manuscript version of this article is solely governed by the terms of such publishing agreement and applicable law.